https://doi.org/10.5194/egusphere-2024-2493
Preprint. Discussion started: 18 September 2024
© Author(s) 2024. CC BY 4.0 License.

Quasi-weekly oscillation of regional $PM_{2.5}$ transport over China driven by the synoptic-scale disturbance of East Asian Winter Monsoon circulation

Yongqing Bai [1], Tianliang Zhao [2,*], Kai Meng [3,*], Yue Zhou [1], Jie Xiong [1], Xiaoyun Sun [4], Lijuan Shen [5], Yanyu Yue [1], Yan Zhu [1], Weiyang Hu [6], Jingyan Yao [2]

[1]China Meteorological Administration Basin Heavy Rainfall Key Laboratory/Hubei Key Laboratory for Heavy Rain Monitoring and Warning Research, Institute of Heavy Rain, China Meteorological Administration, Wuhan 430205, China

[2]Climate and Weather Disasters Collaborative Innovation Center, Key Laboratory for Aerosol-Cloud-Precipitation of China Meteorological Administration, Nanjing University of Information Science &Technology, Nanjing 210044, China

[3]Key Laboratory of Meteorology and Ecological Environment of Hebei Province, Hebei Provincial Institute of Meteorological Sciences, Shijiazhuang, 050021, China

[4]Anhui Province Key Laboratory of Atmospheric Science and Satellite Remote Sensing, Anhui Institute of Meteorological Sciences, Hefei 230031, China

[5]School of Atmosphere and Remote Sensing, Wuxi University, Wuxi, 214105, China

[6]State Key Laboratory of Pollution Control and Resource Reuse and School of the Environment, Nanjing University, Nanjing 210023, China

Correspondence to: Tianliang Zhao (tlzhao@nuist.edu.cn) and Kai Meng (macka@foxmail.com)

Abstract: The regional $PM_{2.5}$ transport is one of the important causes for atmospheric environment change. However, the variations of regional $PM_{2.5}$ transport in synoptic scale with meteorological drivers have been incomprehensively understood. Therefore, this study is targeted at the quasi-weekly oscillation (QWO) of regional $PM_{2.5}$ transport over central and eastern China (CEC) with the influence of synoptic-scale disturbance of the East Asian Winter Monsoon (EAWM) circulation. By constructing the data of daily $PM_{2.5}$ transport flux in CEC in the winters of 2015-2019, we utilize the extended empirical orthogonal function (EEOF) decomposition and other statistical methods to extract the moving spatial distribution of regional $PM_{2.5}$ transport over CEC, recognizing the QWO in regional $PM_{2.5}$ transport with the spatial-temporal variations over CEC. The source-acceptor relationship in regional transport of $PM_{2.5}$ is identified with the 2-d lag effect of the North China Plain, as the upwind source region, on the $PM_{2.5}$ pollution change in the Twain-Hu Basin, as the downwind receptor region in central China. The QWO of regional $PM_{2.5}$ transport over CEC is regulated by the synoptic-scale disturbance of the EAWM circulation with the periodic activities of Siberian high. These findings could provide new insight into the

https://doi.org/10.5194/egusphere-2024-2493
Preprint. Discussion started: 18 September 2024
© Author(s) 2024. CC BY 4.0 License.

understanding of regional $PM_{2.5}$ transport with source-receptor relationship and the meteorological mechanism in atmospheric environment change.

Key words: regional $PM_{2.5}$ transport, quasi-weekly oscillation, source-receptor relationship, extended empirical orthogonal function (EEOF)

1 Introduction

$PM_{2.5}$ pollution has attracted worldwide attention due to its adverse impact on the environment and human health (Agarwal et al., 2017; Fan et al., 2016; Geng et al., 2021; Lin et al., 2018). The $PM_{2.5}$ pollution in the cold season has become one of the major atmospheric environmental problems in China (An et al, 2019; X. Huang et al, 2020). The high-concentration $PM_{2.5}$ tends to occur with extensive spatiotemporal coverage (Tao et al, 2016; Zhang et al, 2019), and synthetic physical-chemical processes caused such heavy $PM_{2.5}$ pollution events (Ding et al, 2017; Quan et al., 2020), including emissions (Liu et al, 2016; Zheng et al, 2018), chemical formation (Huang et al, 2014; Nie et al, 2014), atmospheric boundary layer processes (Huang et al, 2018; Zhong et al, 2019), localized circulation (Miao et al, 2015; Shu et al, 2021; Zheng et al, 2018), as well as weather and climate (Cai et al, 2017; Wu et al, 2016). The interactions among these physical and chemical processes make it more challenging to comprehend the severe haze formation, which serves as one of the major difficulties in forecasting and controlling atmospheric environment change and heavy air pollution (Zhang et al., 2012; Zhang et al., 2019).

$PM_{2.5}$ is featured with complex spatiotemporal changes on multiscale (Georgoulias and Kourtidis, 2012; Wu et al, 2021). $PM_{2.5}$ oscillates periodically at multi-time scales, and the periodic oscillation of atmospheric circulation is the leading cause of the cyclical variations of $PM_{2.5}$ (Chen et al, 2020; Dong et al, 2021; Fu et al, 2020; Perrone et al, 2018). To be specific, the 1-d periodic change or diurnal variation of near-surface $PM_{2.5}$ concentrations is mainly attributed to the atmospheric boundary layer process and localized circulation (Miao et al, 2019); the periodic change of around 7 days may be controlled by the fluctuation of the long-wave trough in middle and high latitudes (Guo et al, 2014); the oscillating cycle of about 14 days is closely related to the quasi-biweekly oscillation of the synoptic circulation (Gao et al, 2020; Zhao et al, 2019); and the 30-60-d intra-seasonal oscillation is mainly caused by the impact of monsoon

https://doi.org/10.5194/egusphere-2024-2493
Preprint. Discussion started: 18 September 2024
© Author(s) 2024. CC BY 4.0 License.

circulation change (Xu et al, 2014; Zhang et al, 2019). Comprehensively revealing the interaction between $PM_{2.5}$ and meteorology at different time scales is essential for solving air pollution problems more effectively (Bäumer and Vogel, 2007; Wang et al, 2020). Previous studies mainly focused on the multiscale periodic variation of atmospheric pollutants in a certain region or local area, not yet found on the $PM_{2.5}$ trans-regional and periodic oscillation in the large area of central and eastern China (CEC).

East Asian Winter Monsoon (EAWM) is the most active atmospheric circulation system in the cold season over the Northern Hemisphere (Ding et al, 2017; Wu and Wang, 2002), which is also a critical leading factor for the variation of wintertime air pollution in CEC (Chin, 2012; Li et al, 2016). Being the major circulation system of EAWM, the Siberian High dominates the cold seasons, acting as a particular driver of cold airflows, so having an important impact on the wintertime atmospheric environment in CEC (An et al, 2019; Shen et al, 2021, 2022; Wu et al, 2016). The strong cold air coming from the Siberian region can effectively remove the air pollutants for the regional transport over China, and a weak Siberian High with the slow southward advance of the cold air is especially favorable for the southerly transport of air pollutants from polluted northern regions in CEC (Hou et al., 2020; Zhang, et al., 2016). When the position of Siberian High is more eastern than normal, the transport of air pollutants from northern China to the south is weakened, and the aggravation of pollution is enhanced in northern China (Jia et al., 2015). Regional pollutant transport driven by the southward movement of a cold front with the Siberian High would exacerbate the air quality in the corresponding receptor regions (Kang et al., 2019; Hu et al., 2021; Shen et al, 2022). The characteristics of atmospheric circulation anomalies favoring heavy haze pollution in China have changed in recent years, and the leading formation mechanism of severe haze has been shifting from local accumulation to regional transport processes in eastern China (Y. Yang et al, 2021). Therefore, studying the influence of EAWM circulation system on regional pollutant transport over CEC is an important issue in atmospheric environment changes (Bai et al, 2021, 2022; Ge et al, 2018; Merrill and Kim, 2004; Tan et al, 2021; W. Yang, et al, 2021).

In recent decades, observational studies reveal the frequent haze in CEC corresponding to a "susceptibility zone" (Xu et al., 2016; Zhu et al, 2018). Anticyclones and cyclones alternatively affect the region on a time scale of 3-7 days, resulting in periodic air pollution in cities (Guo et al.,

https://doi.org/10.5194/egusphere-2024-2493
Preprint. Discussion started: 18 September 2024
© Author(s) 2024. CC BY 4.0 License.

2014). Thus, the weather system in the CEC is basically characterized by periodic changes and the cold air in winter with EAWM oscillates in quasi-weekly periods (Wu and Wang, 2002; Wu et al., 2016). However, the influence of the synoptic-scale disturbance of the EAWM on regional $PM_{2.5}$ transport over CEC is not yet clear. Responding to this problem, this study aims to reveal from a new perspective the quasi-weekly oscillation (QWO) of regional $PM_{2.5}$ transport over CEC affected by EAWM and its underlying mechanism with the synoptic-scale oscillation of the EAWM circulation. This study could be beneficial to deepen the understanding of regional $PM_{2.5}$ transport, its source-receptor relationship and meteorological mechanism in the atmospheric environment changes, and provide scientific evidence for air pollution forecast, early warning and coordinated control.

2 Data and methods

2.1 Environmental and meteorological data

The daily dataset of $PM_{2.5}$ concentrations selected for this study was from China National Environmental Monitoring Center (http://datacenter.mee.gov.cn/), including daily $PM_{2.5}$ concentrations from 1079 air quality monitoring stations in CEC during the winters (December-February) of 2015-2019.

Meteorological data were selected out of the NCEP/NCAR global reanalysis daily data (https://psl.noaa.gov/data/gridded/tables/daily.html) with a grid resolution of 2.5°×2.5° for the large-scale circulation analysis. It is composed of the daily sea level pressure (SLP), air temperature at 1000 hPa, and the U- and V-components of wind at 1000 hPa during the winters of 2015–2019.

In addition, the ERA5-land high-resolution reanalysis hourly dataset (https://cds.climate.copernicus.eu/cdsapp#!/dataset/reanalysis-era5-land?tab=form) with spatial resolution of 0.1°×0.1° was selected for the calculation of transport flux (TF) of $PM_{2.5}$ in CEC. The U- and V-components of the 10-m wind over CEC were obtained from the observations 4 times a day at 00, 06, 12, and 18 UCT in the winter (December-February) of 2015-2019. In order to match the resolution of $PM_{2.5}$ daily data, the ERA5-Land high-resolution 10-m wind was processed into daily average data.

https://doi.org/10.5194/egusphere-2024-2493
Preprint. Discussion started: 18 September 2024
© Author(s) 2024. CC BY 4.0 License.

2.2 $PM_{2.5}$ TF and its divergence

In order to quantitatively characterize the horizontal transport direction and intensity of $PM_{2.5}$ as well as convergence or divergence during regional $PM_{2.5}$ transport, we introduced the concepts of $PM_{2.5}$ TF and divergence of $PM_{2.5}$ TF. Generally, there are two types of TF: horizontal and vertical. This study only addresses the near-surface horizontal $PM_{2.5}$ TF. The horizontal $PM_{2.5}$ TF is defined as the $PM_{2.5}$ mass concentrations passing through the unit area in unit time (unit: μg m^{-2} s^{-1}), expressed as the product of wind vector and $PM_{2.5}$ concentration (Liu et al., 2019; Ma et al., 2021), and its vector points to the same direction as the horizontal wind. The zonal component (F_u) and meridional component (F_v) of $PM_{2.5}$ TF vector (TFV) and the magnitude (TFM) are calculated as follows:

$$F_u = C\,u \quad (1)$$

$$F_v = C\,v \quad (2)$$

$$TFV = F_u\, i + F_v\, j \quad (3)$$

$$TFM = \sqrt{F_u^2 + F_v^2} \quad (4)$$

where C is the surface $PM_{2.5}$ concentration, u and v are the zonal and meridional components of the 10-m wind speed, respectively.

Firstly, the U- and V-components of ERA5-Land high-resolution 10-m wind are interpolated to 1079 stations of environmental measurements in CEC for calculations of near-surface $PM_{2.5}$ TF in this study. Then, the daily $PM_{2.5}$ TF of the 1079 stations for the winters from 2015 to 2019 are calculated according to the calculation by Formulas (1)–(4).

The divergence of $PM_{2.5}$ TF can be an indicator for the $PM_{2.5}$ budget. When positive divergence occurs, the air pollutants were net outflow from the domain region, and vice versa (Wang et al., 2021). The divergence of horizontal $PM_{2.5}$ TF near the surface is calculated as follows (Wang et al., 2021):

$$D = \frac{\partial F_u}{\partial x} + \frac{\partial F_v}{\partial y} \quad (5)$$

where D is the horizontal $PM_{2.5}$ TF divergence, unit: μg m^{-3} s^{-1}. If D is positive (negative), it indicates divergence (convergence) of $PM_{2.5}$ TF.

In the i and j grids, the expression of Formula (5) for the differential calculation with grid

https://doi.org/10.5194/egusphere-2024-2493
Preprint. Discussion started: 18 September 2024
© Author(s) 2024. CC BY 4.0 License.

spacing to be d is

$$D = \frac{Fu_{i+1,j} - Fu_{i-1,j} + Fv_{i,j+1} - Fv_{i,j-1}}{2d} \quad (6)$$

When calculating the horizontal divergence of transport $PM_{2.5}$ flux, it is necessary to interpolate the station data of zonal and meridional components (F_u, F_v) of $PM_{2.5}$ TFV to grid points with 0.25×0.25 grid spacing in CEC and then calculate the divergence of $PM_{2.5}$ TF at each grid point according to Formula (6).

2.3 Butterworth filter

The Butterworth filter is a signal-processing filter to smooth and monotonically reduce the amplitude when the frequency increases without oscillations (Yang et al., 2024). It can extract the changes of variables at different time scales, and thus has been widely applied in climate and meteorology analyses (Gouirand et al., 2012; Yang et al., 2024). In this study, to investigate the QWO (8-d) of regional $PM_{2.5}$ transport over CEC with the influence of EAWM circulations in the synoptic scale, the Butterworth band-pass filtering is performed on the daily $PM_{2.5}$ TFM anomalies and the daily SLP anomalies in the winters of 2015-2019 at quasi-weekly (6-9 days) synoptic-scale component.

2.4 Extended empirical orthogonal function (EEOF)

The Empirical Orthogonal Function (EOF) analysis is a widely-applied climate statistical method in atmospheric and oceanographic scientific studies (Kim et al., 2015; Li et al., 2019; Schepanski et al., 2016), also used to investigate the variability of atmospheric aerosols at different spatiotemporal scales (Bai et al., 2022; Feng et al., 2020). The mathematical process of EOF analysis is to decompose the variable field $X_{m\times n}$, which consists of observation at n times at m spatial points, into a linear combination of p spatial eigenvectors (modes) with corresponding time-weighting coefficients:

$$X_{m\times n} = V_{m\times p} \; T_{p\times n} \quad (7)$$

where V is the spatial eigenvector (load) and T represents the time coefficient. The main information of variable field $X_{m\times n}$ is represented by several eigenvectors. Since the method has been maturely applied, the detailed calculation steps of EOF decomposition are omitted here, and

https://doi.org/10.5194/egusphere-2024-2493
Preprint. Discussion started: 18 September 2024
© Author(s) 2024. CC BY 4.0 License.

our focus is on how to construct the observation matrix.

Firstly, we decompose the daily $PM_{2.5}$ TFM anomalies of 1079 stations in CEC during the winters of 2015-2019 by EOF method. Thus, the following observation matrix can be obtained:

$$X = \begin{bmatrix} x_{11} \cdots x_{1n} \\ \vdots \\ x_{m1} \cdots x_{mn} \end{bmatrix} \tag{8}$$

where X represents the $PM_{2.5}$ TFM anomalies, m represents the spatial points for 1079 stations, and n represents the observation times of 450 days. Then, the variable field X is decomposed into the sum of the product of space and time functions according to Formula (7).

EOF decomposition of $PM_{2.5}$ TFV anomalies can be performed by employing the complex matrix, hence the following observation matrix is constructed:

$$X = \begin{bmatrix} u_{11} \cdots u_{1n} \\ \vdots \\ u_{m1} \cdots u_{mn} \\ v_{11} \cdots v_{1n} \\ \vdots \\ v_{m1} \cdots v_{mn} \end{bmatrix} \tag{9}$$

where X is the $PM_{2.5}$ TFV anomalies, and u and v refer to the zonal and meridional components of TFV anomalies.

With EOF analysis we can get the spatial distribution structure, which is in a fixed time pattern of climate variables, but we cannot get a temporally moving spatial distribution structure. By using the autocorrelation existing in the time of variable and selecting lag time, the extended EOF (EEOF) analysis is an EOF-based method designed for extending the original observation matrix into multiple extended matrices over continuous times to obtain moving spatial distribution structure of variable. This method has found widespread applications in the analysis and prediction of marine and atmospheric motions (Dey et al., 2018; Qian et al., 2019; H. Wang et al., 2019).

In this study, we utilized the EEOF analysis to reveal the evolution of $PM_{2.5}$ TF to reveal the spatiotemporal variations of regional $PM_{2.5}$ transport. On the basis of Formula (8), a new extension matrix of $PM_{2.5}$ TFM is constructed. Due to the study on the synoptic scale, 5 lag times are selected, and each lag time is 1 day in length. The constructed observation matrix is as follows:

https://doi.org/10.5194/egusphere-2024-2493
Preprint. Discussion started: 18 September 2024
© Author(s) 2024. CC BY 4.0 License.

$$X = \begin{bmatrix} X_{1,1} \cdots X_{1,n-5} \\ \vdots \\ X_{m,1} \cdots X_{m,n-5} \\ X_{1,2} \cdots X_{1,n-4} \\ \vdots \\ X_{m,2} \cdots X_{m,n-4} \\ X_{1,3} \cdots X_{1,n-3} \\ \vdots \\ X_{m,3} \cdots X_{m,n-3} \\ X_{1,4} \cdots X_{1,n-2} \\ \vdots \\ X_{m,4} \cdots X_{m,n-2} \\ X_{1,5} \cdots X_{1,n-1} \\ \vdots \\ X_{m,5} \cdots X_{m,n-1} \\ X_{1,6} \cdots X_{1,n} \\ \vdots \\ X_{m,6} \cdots X_{m,n} \end{bmatrix} \quad (10)$$

Seen from Formula (10), the new extended matrix is composed of $X_{6m,n-5}$, where X is the $PM_{2.5}$ TFM anomalies, m is the spatial points of observation station, and n is the observation times of 450 days. When EEOF decomposition is performed on $PM_{2.5}$ TFV, the complex matrix is still used for the extension, and the same lag scheme is adopted to construct a new extended matrix of $PM_{2.5}$ TFV based on Formula (9). After constructing the initial data matrix, the EEOF decomposition method is in line with the classical EOF decomposition method.

3 Results and discussion

3.1 QWO of regional $PM_{2.5}$ transport over CEC

The EOF decomposition is carried out on the daily anomalies of $PM_{2.5}$ TFM and TFV in the winters of 2015-2019 over CEC. The first two EOFs explain 26.6% and 14.2% (29.1% and 11.8%) of the total anomalous variations of $PM_{2.5}$ TFM (TFV), which is very helpful for better characterizing regional $PM_{2.5}$ transport variations.

Two principal modes govern the variations of $PM_{2.5}$ TF anomalies over CEC: the first leading

https://doi.org/10.5194/egusphere-2024-2493
Preprint. Discussion started: 18 September 2024
© Author(s) 2024. CC BY 4.0 License.

mode of monopole (EOF1) and the second mode of meridional dipole (EOF2) (Fig. 1). EOF1 indicates the enhanced $PM_{2.5}$ TF over CEC (Fig. 1a). The large value center of TF mainly occurs in central China, and the transport vector direction is abnormally by north. The horizontal $PM_{2.5}$ transport is unusually strong in central China affected by the EAWM, presenting a typical channel for regional $PM_{2.5}$ transport over CEC (Yang W. et al., 2021). The dipole mode of $PM_{2.5}$ TF anomalies displays a south–north out-of-phase pattern, with the flux large value centers located in the North China Plain (NCP) and the Twain-Hu Basin (THB) respectively, and the vector directions are opposite (Fig. 1b). This mode indicates that the air pollutants from NCP in the upwind are transported to THB in the downwind driven by the prevailing northerlies of EAWM (Hu et al., 2021; Shen et al., 2022), and the $PM_{2.5}$ flux in NCP decreases while that in THB increases in the regional $PM_{2.5}$ transport process.

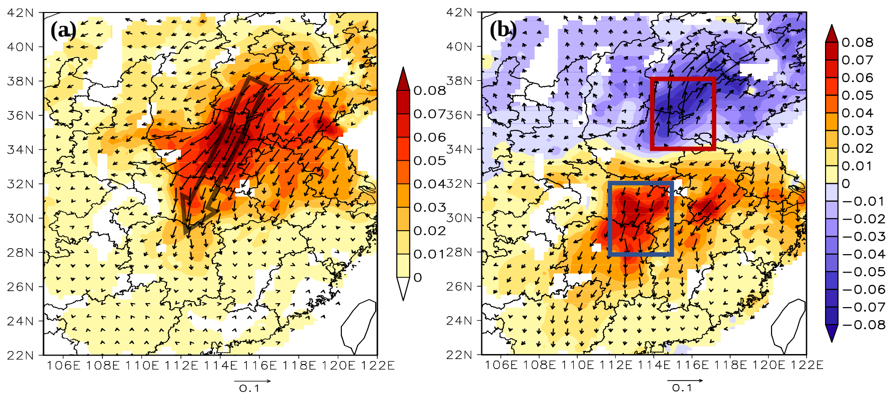

Figure 1. Spatial pattern of the (a) EOF1 and (b) EOF2 loads in the daily change of $PM_{2.5}$ TFV anomalies (vectors) and TFM anomalies (color contours) over CEC in the winters of 2015-2019. The red and blue boxes indicate NCP and THB, respectively.

Through EOF decomposition, the $PM_{2.5}$ TF could be understood from the perspective of a fixed time pattern of climate, but the spatial structure with $PM_{2.5}$ TF over CEC failed to be obtained. However, EEOF decomposition can be used to analyze the continuous structural evolution of the main modes of regional $PM_{2.5}$ TF over CEC.

The EEOF decomposition was carried out for the daily variations of $PM_{2.5}$ TFM anomalies and TFV anomalies respectively over CEC during the winters of 2015-2019. Figure 2 and Figure

https://doi.org/10.5194/egusphere-2024-2493
Preprint. Discussion started: 18 September 2024
© Author(s) 2024. CC BY 4.0 License.

S1 show the spatial distribution of different lag times for the main modes of EEOFs, which account for about 20% of the total variation. According to the analysis, the $PM_{2.5}$ TFM anomalies for EEOF2 and EEOF3, as well as TFV anomalies for EEOF1 and EEOF2, all show the structural evolutions in the different phases of regional $PM_{2.5}$ transport in one cycle. As it can be seen, Figures. 2a-d, S1a-d, and 2e-h respectively describe the evolution of the first and second four phases in a cycle and the first four phases in the next cycle (one phase represents 1day).

Figures 2a-d illustrate the positive anomalies of $PM_{2.5}$ TF shifting from NCP to THB in the first four phases under the effect of the EAWM, causing the upwind $PM_{2.5}$ TF to decrease and the downwind $PM_{2.5}$ TF to increase, which is in line with the spatial pattern of the EOF modes in Figure 1. The last four phases show the out-of-phase pattern of the first half cycle (Figs. S1a-d). It is noted that when anomalies of $PM_{2.5}$ TFV in the NCP turn to the northerly direction (Fig. S1d and Fig. 2e), it is a strong signal initiating the regional $PM_{2.5}$ transport. Then, the transport is repeated in the next periodic cycle (Figs. 2e-h). Therefore, the regional $PM_{2.5}$ transport over CEC enjoys a quasi-weekly (8-d) oscillation pattern.

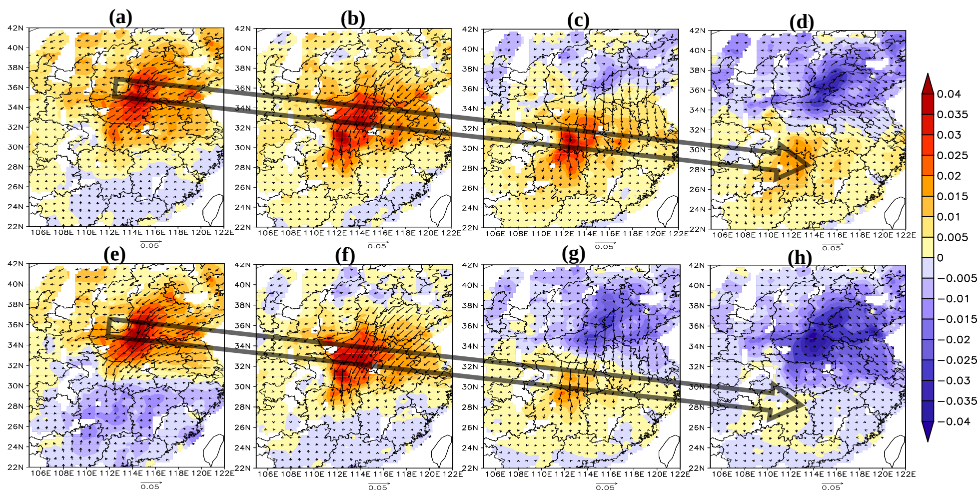

Figure 2. (a)-(d) The first four phases (days) of QWO (8-d) during the regional $PM_{2.5}$ transport over CEC; (e)-(h) the first four phases (days) of the next cycle. The Loads of $PM_{2.5}$ TFM anomalies (color contours) for EEOF2 and TFV anomalies (vectors) for EEOF1 with lag time (a) 0 d, (b)1 d, (c) 2 d and (d) 3 d, and loads of TFM anomalies (color contours) for EEOF3 and TFV anomalies (vectors) for EEOF2 with lag time (e) 2 d, (f) 3 d, (j) 4 d and (h) 5 d over CEC in the winters of 2015-2019.

https://doi.org/10.5194/egusphere-2024-2493
Preprint. Discussion started: 18 September 2024
© Author(s) 2024. CC BY 4.0 License.

To further study the variations of regional $PM_{2.5}$ transport over CEC, we have screened out 23 typical events with greater than 1.5 times standard deviations based on the standardized time coefficient of EEOF, and then used the 8 consecutive days of each event as the 8 phases of QWO in the composite analysis on the 23 typical events of regional $PM_{2.5}$ transport over CEC.

Figure 3 shows the composited $PM_{2.5}$ TF, divergence of $PM_{2.5}$ TF, and $PM_{2.5}$ concentration anomalies in the first four phases of QWO. The high fluxes of $PM_{2.5}$ transport from north to south persists for 3-4 days over CEC and decline in the THB (Fig. 3a-d). The regional $PM_{2.5}$ transport lifetime corresponding to synoptic systems is about 3-5 days (H. Huang et al., 2020). Abnormal northerly winds drive the heavy $PM_{2.5}$ pollution from the upwind NCP to the downwind regions, aggravating $PM_{2.5}$ pollution in the downwind THB (Figs. 3e-h). It is noteworthy that the regions $PM_{2.5}$ TF convergence zone (negative value of divergence) matches spatially the centers positive anomaly centers of $PM_{2.5}$ concentrations, which is confirmed with a significantly negative correlation of the $PM_{2.5}$ concentrations with divergences of $PM_{2.5}$ TF in the 23 typical events (Fig. S2). The $PM_{2.5}$ transport is accompanied by flux convergence, which is beneficial to the $PM_{2.5}$ accumulation. In addition, the $PM_{2.5}$ TF in the upwind NCP changes from convergence to divergence, and the divergence of the $PM_{2.5}$ TF in the downwind THB alters to convergence in the meantime (Figs. 3i-l), indicating that the $PM_{2.5}$ over THB is transported from the upwind NCP. The source-receptor relationship between NCP and THB during the regional $PM_{2.5}$ transport over CEC is discussed in detail in the next section.

https://doi.org/10.5194/egusphere-2024-2493
Preprint. Discussion started: 18 September 2024
© Author(s) 2024. CC BY 4.0 License.

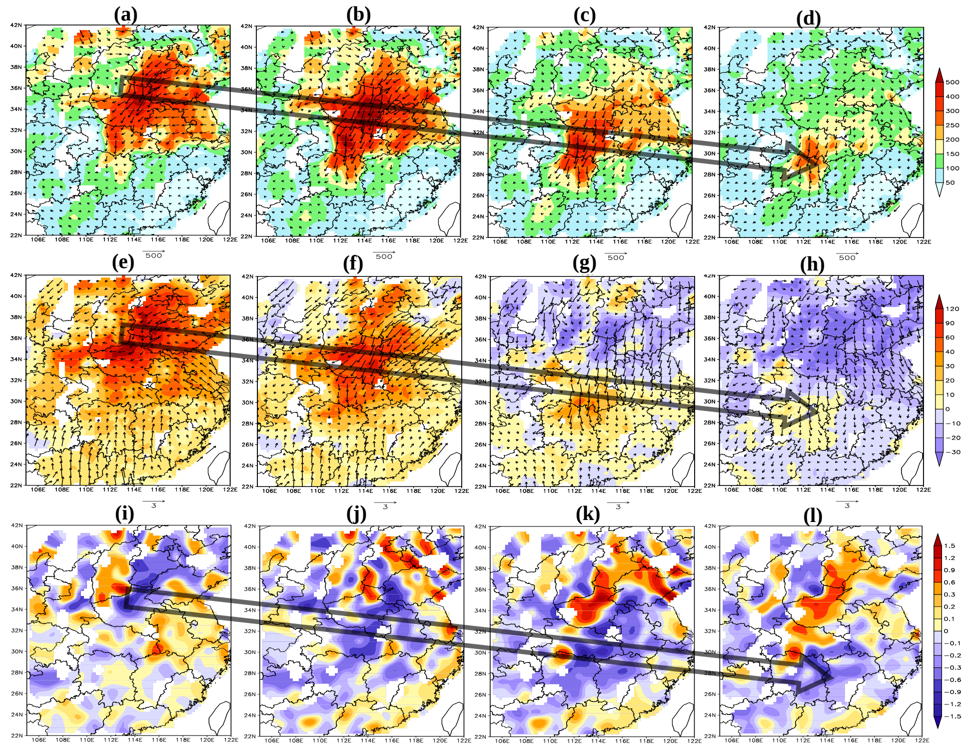

Figure 3. Spatial distributions of the composited (a-d) $PM_{2.5}$ TFM (color contours, unit: μg m^{-2} s^{-1}) and TFV (vectors, unit: μg m^{-2} s^{-1}), (e-h) anomalies of $PM_{2.5}$ concentrations (color contours, unit: μg m^{-3}) and 10-m wind vectors (unit: m s^{-1}), (i-l) divergence of $PM_{2.5}$ flux (color contours, unit: 10^{-3}μg m^{-3} s^{-1}) in the first four phases of QWO during the 23 typical events of regional $PM_{2.5}$ transport over CEC.

3.2 Source-receptor relationship in regional $PM_{2.5}$ transport from NCP to THB

The regional pollutant transport governed by emissions and meteorology leads to a complex source–receptor relationship of air pollution changes (Yu et al., 2020). Band-pass filtering is performed on the daily $PM_{2.5}$ TFM anomalies at a quasi-weekly (6-9 days) synoptic scale in the winters of 2015-2019. In Figure 4a, we composite the filter components of $PM_{2.5}$ TFM in the 8 phases of QWO during the 23 typical events of regional $PM_{2.5}$ transport over the NCP and THB, respectively. The $PM_{2.5}$ TF exhibits an obvious QWO on the synoptic scale (Fig. 4a). The $PM_{2.5}$ TF over the NCP continues to decline in the first four phases, while that of THB first rises and then falls in the last four phases, the $PM_{2.5}$ TF over the NCP increases continuously, while that of

https://doi.org/10.5194/egusphere-2024-2493
Preprint. Discussion started: 18 September 2024
© Author(s) 2024. CC BY 4.0 License.

THB falls first and then rises. We can see that the QWO of $PM_{2.5}$ TF over THB lags behind the NCP by 2 phases (Fig. 4a). The high TFM of $PM_{2.5}$ from NCP in the first phase spread to THB, resulting in the peak of $PM_{2.5}$ TF over THB in the third phase.

In addition, the distribution of the differences in $PM_{2.5}$ TF and the vectors between phase 3 and phase 1 of the QWO, and the $PM_{2.5}$ TF decrease and increase from phase 1 to phase 3 respectively over the upwind NCP and the downwind THB, which is in accordance with the spatial pattern of the EOF mode (Figs.1b and 4b), indicating that the source-receptor relationship over CEC exist the regions NCP and THB of regional $PM_{2.5}$ transport over CEC.

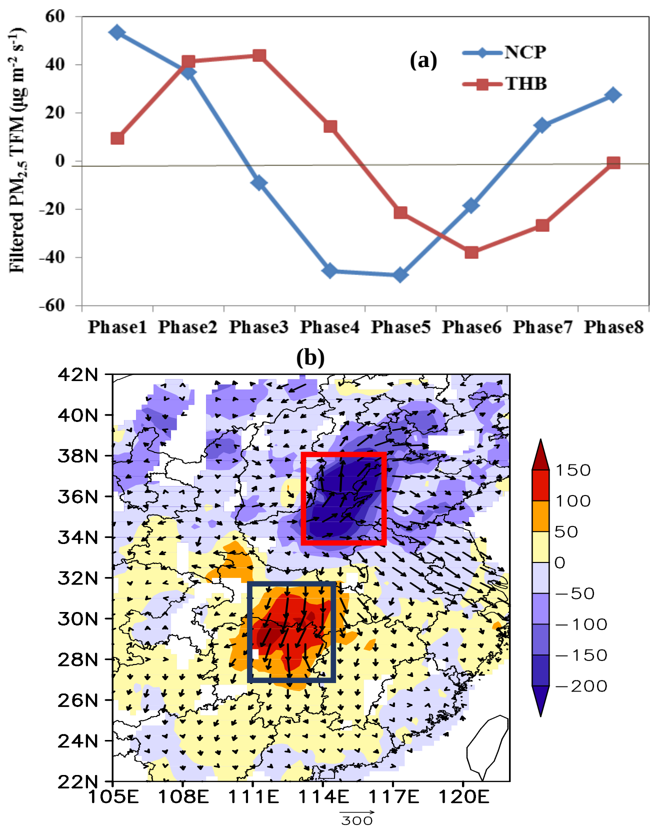

Figure 4. (a) The 8 phases of QWO during the 23 typical events of regional $PM_{2.5}$ transport over the NCP and THB with composited 6-9 d band-pass filtering of $PM_{2.5}$ TFM; (b) spatial distribution of the differences in $PM_{2.5}$ TFM (color contours, unit: μg m^{-2} s^{-1}) and TFV (vectors, unit: μg m^{-2} s^{-1}) between the 3rd phase and the 1st phase of QWO. The red and black boxes represent NCP and THB.

https://doi.org/10.5194/egusphere-2024-2493
Preprint. Discussion started: 18 September 2024
© Author(s) 2024. CC BY 4.0 License.

The statistical analysis based on long-term observation also shows that there is a significant 2-day lag relationship of positive correlation between NCP and THB in $PM_{2.5}$ TF in the QWO (Fig. 5a). This discloses that the air pollutants are transported from the upwind NCP to the downwind THB in 2 days, confirming a quasi-2-d lag in the regional $PM_{2.5}$ transport from NCP to THB (Hu et al., 2021; Shen et al., 2021). Additionally, in the long-term change of air pollution, the divergences of $PM_{2.5}$ TF in the NCP are significantly negatively correlated to that of THB (Fig. 5b), that is, the $PM_{2.5}$ TF convergences in the downwind THB fits well with the $PM_{2.5}$ TF divergence in the upwind NCP. It can be reflected that the changes in the synoptic scale of EAWM atmospheric circulation impel the regional $PM_{2.5}$ transport to build the source-receptor relationship of atmospheric pollutants between the NCP and THB.

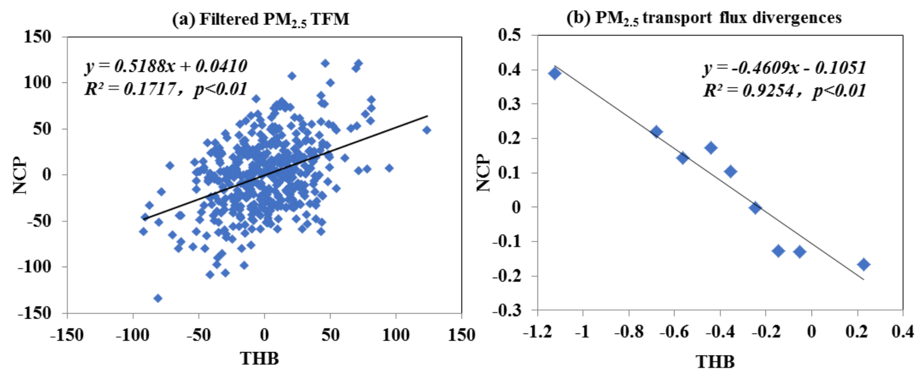

Figure 5. (a) Scatter plot of 6-9-d filtering components of $PM_{2.5}$ TFM (10^{-3} μg m^{-2} s^{-1}) over THB in 2-day lag and NCP during the winters of 2015-2019; (b) scatter plot of $PM_{2.5}$ TF divergences (10^{-3} μg m^{-3} s^{-1}) between THB and NCP, and the $PM_{2.5}$ TF divergences are averaged over the value interval of 0.1.

3.3 Effect of synoptic-scale disturbance of EAWM circulation on QWO of regional $PM_{2.5}$ transport over CEC

Meteorological change is the essential factor in regulating the occurrence and development of $PM_{2.5}$ pollution on synoptic scales. To investigate the QWO of EAWM circulation in the synoptic scale disturbance, this study performs the 6-9-d band-pass filtering of the daily SLP anomalies (denoted as SLP_{QWO}) in East Asia during the winters of 2015-2019. The SLP and SLP_{QWO} fields (Figs. 6-7) as well as $PM_{2.5}$ concentrations and 10-m winds (Fig. S3) in the 8 phases of QWO

https://doi.org/10.5194/egusphere-2024-2493
Preprint. Discussion started: 18 September 2024
© Author(s) 2024. CC BY 4.0 License.

during the 23 typical events were composited, respectively. The QWO of regional $PM_{2.5}$ transport is connected with the "weekly-cycle" synoptic process of $PM_{2.5}$ transport and accumulation over CEC (Fig. S3), and it is powered mainly by the Siberian High circulation with the synoptic-scale disturbance of EAWM circulation (Figs. 6 and 7).

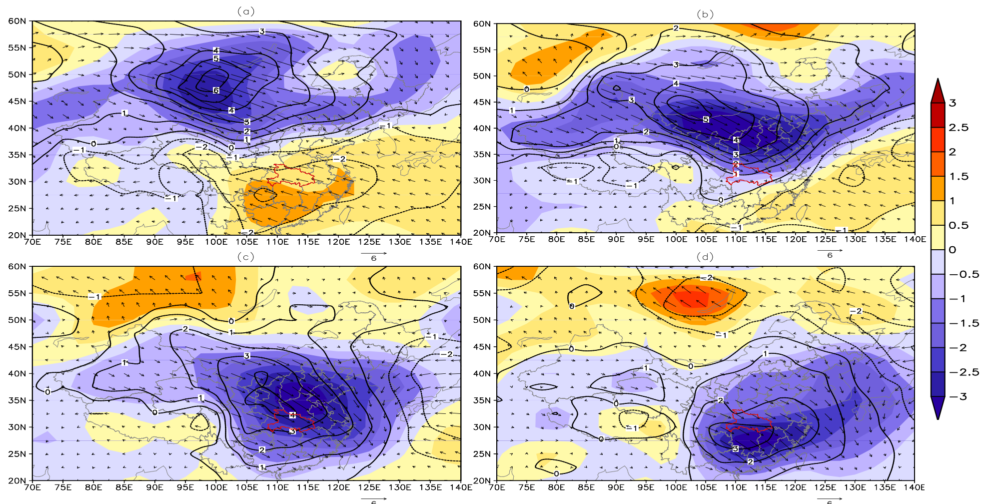

Figure 6. The composited differences between the current day and the previous day of SLP (black contour lines, unit: hPa), 1000 hPa air temperature (color contours, unit:℃) and wind vectors (unit: m s^{-1}) in the first four phases (a-d) of QWO during the 23 typical events.

The condition of uniform pressure in the front of Siberian High could favor the $PM_{2.5}$ accumulation over the NCP for triggering regional $PM_{2.5}$ transport over CEC (Fig. 7a). The regional heavy pollution of $PM_{2.5}$ >150 μg m^{-3} lasts for 1-2 days (Figs. S3a and S3b). With the development of the Siberian High, the extension of the high pressure guides the cold air to advance southward (Park et al., 2014). As the result of the increasing air pressure gradients, the strong northerly winds in the EAWM circulation system, deliver high-level $PM_{2.5}$ air mass from NCP to THB (Figs. 7a-d, Figs. S3a-d). In addition, the cold and high air pressure system with the abnormal northerly airflows moves from the Siberia-Mongolia region to CEC in the first four phases (Fig. 6), providing beneficial synoptic circulation patterns for regional $PM_{2.5}$ transport. Thus, the periodic extension of the Siberian High with the associated strong cold air intrusion is an important driver in the regional $PM_{2.5}$ transport over CEC.

https://doi.org/10.5194/egusphere-2024-2493
Preprint. Discussion started: 18 September 2024
© Author(s) 2024. CC BY 4.0 License.

Notably, we can see that in the first four phases, the SLP_{QWO} positive anomalies occur, develop, and expand southward from the Siberia-Mongolia region to CEC (Figs. 7a-d). The synoptic-scale disturbance with the extension of Siberian High and the southward movement of cold air could drive the regional $PM_{2.5}$ transport over CEC (Figs. 7a-d). The situation of the last four phases is opposite to the SLP_{QWO} negative anomalies in Siberia-Mongolia region, inhibiting the Siberian High and cold air intrusion (Figs. 7e-h). The low and uniform pressure is beneficial to the accumulation of $PM_{2.5}$. Therefore, the periodic changes in the synoptic-scale disturbance of the EAWM circulation impel the QWO of regional $PM_{2.5}$ transport over CEC.

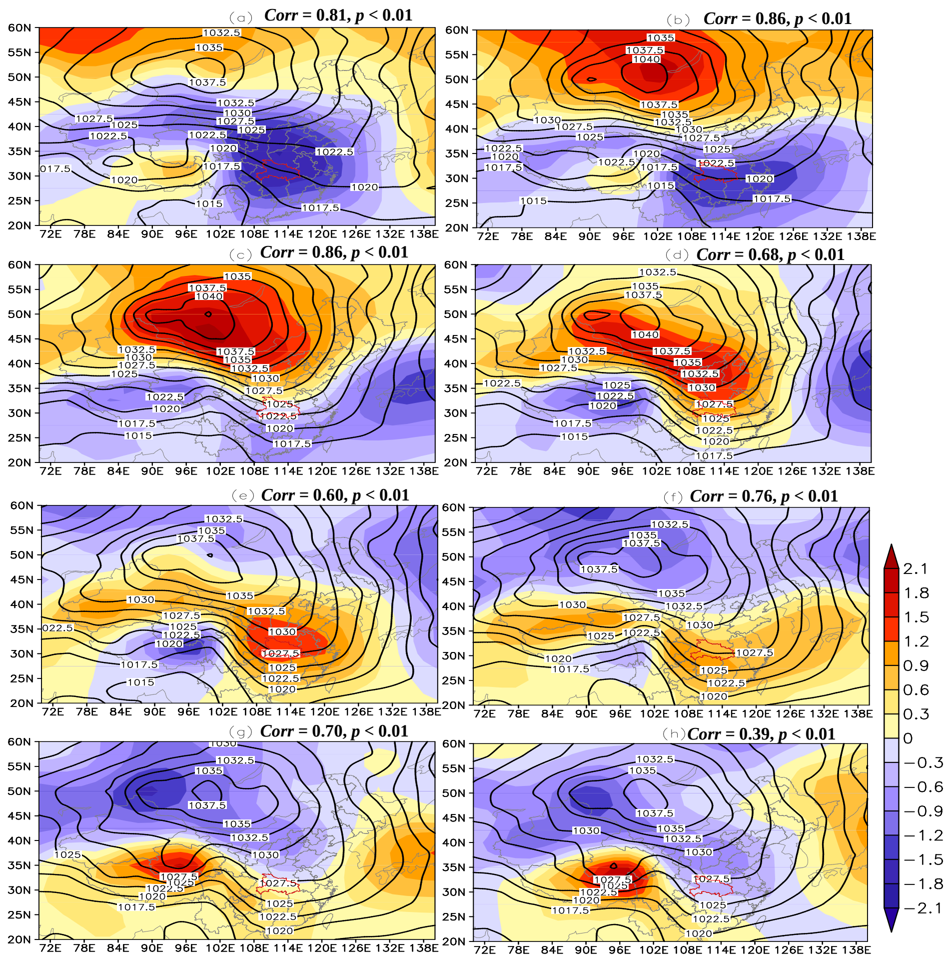

Figure 7. Composited SLP (black contour lines, unit: hPa) and its synoptic-scale filter component SLP_{QWO} (color

https://doi.org/10.5194/egusphere-2024-2493
Preprint. Discussion started: 18 September 2024
© Author(s) 2024. CC BY 4.0 License.

contours, unit: hPa) in the 8 phases (a-h) of QWO during the 23 typical events. *Coor* represents the spatial correlation coefficients between SLP_{QWO} and the load of SLP_{QWO} decomposed by EEOF in Fig. S4.

In addition, the EEOF decomposition is carried out on the SLP_{QWO} field in the winters of 2015-2019 to recognize the periodic activities in the synoptic scale of the EAWM circulation. The cold air activity of EAWM presents QWO (Wu and Wang, 2002). The positive (negative) synoptic-scale disturbance occurs in the Siberia-Mongolia region, and then spreads to CEC along the northwest-southeast path, contributing to the 8-d cycle of QWO (Fig. S4). Notably, the spatial correlation coefficients between the load of SLP_{QWO} decomposed by EEOF (Fig. S4) and the SLP_{QWO} composited during 23 typical events (Fig.7) are highly positively correlated in the 8 phases, respectively. Therefore, the QWO in the synoptic-scale activities of the Siberian high is an important factor for driving the QWO of regional $PM_{2.5}$ transport over CEC.

4 Conclusions

Exploring the periodical oscillations of $PM_{2.5}$ pollution over CEC and the meteorological effect is crucial for understanding the change in the atmospheric environment and improving regional air quality forecasts. In this study with constructing a dataset of the daily $PM_{2.5}$ TF, the EEOF and statistical methods are used to identify the QWO of regional $PM_{2.5}$ transport with the spatiotemporal variations over CEC in winters from 2015 to 2019. The source-receptor relationship is recognized between NCP and THB with the QWO of regional $PM_{2.5}$ transport over CEC with the typical EAWM climate. Furthermore, it is revealed that the driving effect of synoptic-scale disturbance of EAWM circulations on the QWO of regional $PM_{2.5}$ transport over China.

The variations of $PM_{2.5}$ TF over CEC are dominated by the first leading monopole mode and the second meridional dipole mode. The monopole mode indicates the high $PM_{2.5}$ flux along the channel of regional $PM_{2.5}$ transport from NCP to THB under the governs of the EAWM circulations, and the dipole mode exhibits a pattern of south-north out-phase with two centers existing respectively in the upwind NCP and the downwind THB in regional transport of $PM_{2.5}$ over CEC. In terms of the long-term changes in air pollution of 2015–2019, the regional $PM_{2.5}$ transport over CEC is featured with the QWO, verifying a source-receptor relationship for the

© Author(s) 2024. CC BY 4.0 License.

regional $PM_{2.5}$ transport from NCP to THB in 2 days. Such changes are incurred by the QWO in the activities of the Siberian High, and this synoptic-scale disturbance of the EAWM circulations is generated in the Siberia-Mongolia region, and then develops, marching into CEC, regulating the QWO of regional $PM_{2.5}$ transport.

Based on the 5-winter (2015-2019) observations of $PM_{2.5}$ concentrations and the corresponding meteorological reanalysis data, this study with the climate statistical and diagnostic methods investigates the QWO of regional $PM_{2.5}$ transport in China with the influence of synoptic-scale disturbance of EAWM circulation, providing a new insight into the understanding of regional pollutant transport with meteorological drivers in atmospheric environment changes. Further studies with the fine observations of air pollutants and meteorology in the longer term could explore variations in regional transport of particles and gaseous precursors with their contribution to $PM_{2.5}$ pollution through the artificial intelligence integrating physical and chemical process analysis.

Data availability. All data used in this paper can be provided upon request from Yongqing Bai (2007byq@163.com)

Author contributions. YB and TZ conceived the study. YB designed the graphics and wrote the manuscript with help from TZ, KM, YZ, JX, XS, LS, YY, YZ, WH and JY were involved in the scientific discussion. All authors commented on the paper.

Competing interests. The authors declare that they have no conflict of interest.

Financial support. This research was supported by the National Natural Science Foundation of China (grant no. 42075186, 41830965) and the National Key Research and Development Program of China (2022YFC3701204).

References

Agarwal, N. K., Sharma, P., Agarwal, S. K., 2017. Particulate matter air pollution and cardiovascular disease, Med. Sci. 21, 270–279.

An, Z., Huang, R., Zhang, R., Tie, X., Li, G., Cao, J., Zhou, W., Shi, Z., Han, Y., Gu, Z., Ji, Y., 2019. Severe haze in northern China: A synergy of anthropogenic emissions and atmospheric processes. Proceedings of the National Academy of Sciences of the United States of America 116, 8657–8666.

https://doi.org/10.5194/egusphere-2024-2493
Preprint. Discussion started: 18 September 2024
© Author(s) 2024. CC BY 4.0 License.

Bai, Y., Zhao, T., Zhou, Y., Kong, S., Hu, W., Xiong, J., Liu, L., Zheng, H., Meng, K., 2021. Aggravation effect of regional transport on wintertime $PM_{2.5}$ over the middle reaches of the Yangtze River under China's air pollutant emission reduction process. Atmospheric Pollution Research 12, 101111.

Bai, Y., Zhao, T., Hu, W., Zhou, Y., Xiong, J., Wang, Y., Liu, L., Shen, L., Kong, S., Meng, K., Zheng, H., 2022. Meteorological mechanism of regional $PM_{2.5}$ transport building a receptor region for heavy air pollution over Central China. Sci. Total Environ. 808, 151951.

Bäumer, D., Vogel, B., 2007. An unexpected pattern of distinct weekly periodicities in climatological variables in Germany. Geophysical Research Letters 34, L03819.

Cai, W., Li, K., Liao, H., Wang, H., Wu, L., 2017. Weather conditions conducive to Beijing severe haze more frequent under climate change. Nat. Clim. Chang. 7, 257–262.

Chen, X., Yin, L., Fan Y., Song, L., Ji, T., Liu, Y., Tian, J., Zheng, W., 2020. Temporal evolution characteristics of $PM_{2.5}$ concentration based on continuous wavelet transform, Science of the Total Environment 699, 134244.

Chin M., 2012. Dirtier air from a weaker monsoon. Nat. Geosci. 5, 449–450.

Dey, A., Chattopadhyay, R., Sahai, A. K., Mandal, R., Joseph, S., Phani, R., Abhilash, S., 2018. An operational tracking method for the MJO using extended empirical orthogonal functions, Pure. Appl. Geophys. 176, 2697–2717.

Ding, A., Huang, X., Fu, C., 2017. Air Pollution and Weather Interaction in East Asia, Oxford Research Encyclopedia, 10.1093/acrefore/9780199389414.013.536.

Dong, Y., Zhou, H., Fu, Y., Li, X., Geng, H., 2021. Wavelet periodic and compositional characteristics of atmospheric $PM_{2.5}$ in a typical air pollution event at Jinzhong city, China, Atmospheric Pollution Research 12, 245–254.

Fan, J., Wang, Y., Rosenfeld, D., Liu, X., 2016. Review of aerosol–cloud interactions: Mechanisms, significance, and challenges. J. Atmos. Sci. 73, 4221–4252.

Feng, J., Zhu, J., Li, J., Liao, H., 2020. Aerosol concentrations variability over China: two distinct leading modes. Atmos. Chem. Phys., 20, 9883–9893.

Fu, H., Zhang, Y., Liao C., Mao, L., Wang, Z., Hong, N., 2020. Investigating $PM_{2.5}$ responses to other air pollutants and meteorological factors across multiple temporal scales, Sci. Rep. 10, 15639.

Gao, L., Wang, T., Ren X., Zhuang, B., Li, Shu., Yao, R., Yang, X., 2020. Impact of atmospheric quasi-biweekly oscillation on the persistent heavy $PM_{2.5}$ pollution over Beijing-Tianjin-Hebei region, China during winter, Atmospheric Research 242, 105017.

Ge, B., Wang, Z., Lin, W., Xu, X., Li, J., Ji, D., Ma, Z., 2018. Air pollution over the North China Plain and its implication of regional transport: A new sight from the observed evidences, Environmental Pollution 234, 29–38.

Geng, G., Zheng, Y., Zhang Q., Xue, T., Zhao, H., Tong, D., Zheng, B., Li, M., Liu, F., Hong, C., He, K., Davis, S. J., 2021. Drivers of $PM_{2.5}$ air pollution deaths in China 2002–2017, Nature Geoscience 14, 645–650.

Georgoulias, A. K., Kourtidis, K. A., 2012. A high resolution satellite view of the aerosol weekly cycle variability over Central Europe. Atmospheric Research 107, 145–160.

Gouirand, I., Jury, M.R., Sing, B., 2012. An analysis of low- and high-frequency summer climate variability around the Caribbean Antilles. J. Climate 25, 3942–3952.

Guo, S., Hu, M., Zamora, M. L., Peng, J., Zhang, R., 2014. Elucidating severe urban haze formation in China. Proc. Natl. Acad. Sci. USA. 111, 17373–17378.

Hou, X., Zhu, B., Kumar, K. R., de Leeuw, G., Lu, W., Huang, Q., Zhu, X., 2020. Establishment of conceptual schemas of surface synoptic meteorological situations affecting fine particulate pollution across eastern China in the winter. Journal of Geophysical Research: Atmospheres 125, e2020JD033153.

https://doi.org/10.5194/egusphere-2024-2493
Preprint. Discussion started: 18 September 2024
© Author(s) 2024. CC BY 4.0 License.

Hu, W., Zhao, T., Bai, Y., Kong, S., Xiong, J., Sun, X., Yang, Q., Gu, Y., Lu, H., 2021. Importance of regional $PM_{2.5}$ transport and precipitation washout in heavy air pollution in the Twain-Hu Basin over Central China: Observational analysis and WRF-Chem simulation. Sci. Total. Environ. 758, 143710.

Huang, R. J., Zhang, Y., Bozzetti, C., Ho, K. F., Cao, J. J., Han, Y., Daellenbach. K. R., Slowik, J. G., Platt, S. M., Canonaco, F., Zotter, P., Wolf, R., Pieber, S. M., Bruns, E., A., Crippa, M., Ciarelli, G., Piazzalunga, A., Schwikowski. M., Abbaszade, G., Kreis, J. S., Zimmermann, R., An, Z., Szidat, S., Baltensperger, U., Haddad, I. E., Prevot, A. S. H., 2014. High secondary aerosol contribution to particulate pollution during haze events in China. Nature 514, 218–222.

Huang, X., Wang, Z., Ding, A., 2018. Impact of aerosol-PBL interaction on haze pollution: Multiyear observational evidences in North China. Geophys. Res. Lett. 45, 8596–8603.

Huang, H., Wang, S., Huang, W., Lin, N., Chuang, M., Silva, A. M., Peng. C., 2020. Influence of synoptic-dynamic meteorology on the long-range transport of Indochin biomass burning aerosols. Journal of Geophysical Research: Atmospheres 125, e2019JD031260.

Huang, X., Ding, A., Wang, Z., Ding, K., Gao, J., Chai, F., Fu, C., 2020. Amplified transboundary transport of haze by aerosol–boundary layer interaction in china. Nature Geoscience 13, 428-434.

Jia, B., Wang, Y., Yao, Y., Xie,Y., 2015. A new indicator on the impact of large-scale circulation on wintertime particulate matter pollution over China. Atmos. Chem. Phys. 15, 11919–11929.

Kang, H., Zhu, B., Gao, J., He, Y., Wang, H., Su, J., Pan. C., Zhu, T., Yu, B., 2019. Potential impacts of cold frontal passage on air quality over the Yangtze River Delta, China. Atmos. Chem. Phys. 19, 3673–3685.

Kim, B. H., Ha, K, J., 2015. Observed changes of global and western Pacific precipitation associated with global warming SST mode and mega-ENSO SST mode. Clim. Dynam. 45, 3067–3075.

Li, Q., Zhang, R., Wang, Y., 2016. Interannual variation of the wintertime fog-haze days across central and eastern China and its relation with EAWM. Int. J. Climatol. 36, 346–354.

Li, X., Gereon, G., Greatbatch, R. J., Lu, R., 2019. Impact of the MJO on the interannual variation of the Pacific–Japan mode of the East Asian summer monsoon. Clim. Dynam. 52, 3489–3501.

Lin, Y., Zou, J., Yang, W., and Li, C. Q., 2018. A Review of Recent Advances in Research on $PM_{2.5}$ in China, Int., J., Env., Res., Pub., He. 15, 438.

Liu, J., Mauzerall, D. L., Chen, Q., Zhang, Q., Song, Y, Peng, W., Klimont. Z., Qiu, X., Zhang, S., Hu, M., Lin, W., Smith, K. R., Zhu, T., 2016. Air pollutant emissions from Chinese households: A major and underappreciated ambient pollution sources. P. Natl. Acad. Sci. USA. 113, 7756–7761.

Liu, Y., Tang, G., Zhou, L., Hu, B., Liu, B., Li, Y., Liu, S., Wang, Y., 2019. Mixing layer transport flux of particulate matter in Beijing, China. Atmos. Chem. Phys. 19, 9531–9540.

Ma, Y., Zhu, Y., Liu, B., Li, H., Jin, S., Zhang, Y., Fan, R., Gong, W. 2021. Estimation of the vertical distribution of particle matter ($PM_{2.5}$) concentration and its transport flux from lidar measurements based on machine learning algorithms. Atmos. Chem. Phys. 21, 17003–17016.

Merrill, J. T., Kim, J., 2004. Meteorological events and transport patterns in ACE-Asia. Journal of Geophysical Research Atmospheres 109, D19S18.

Miao, Y., Hu, X.M., Liu, S., Qian, T., Xue, M., Zheng, Y., Wang, S., 2015. Seasonal variation of local atmospheric circulations and boundary layer structure in the Beijing-Tianjin-Hebei region and implications for air quality. J. Adv. Model. Earth Sys. 7, 1602–1626.

Miao, Y., Li, J., Miao, S., Che, H., Wang, Y., Zhang, X., Zhu, R., Liu, S., 2019. Interaction between planetary boundary layer and $PM_{2.5}$ pollution in megacities in China: a review. Curr. Pollut. Rep. 5, 261–271.

Nie, W., Ding, A., Wang, T., Kerminen, V. M., George, C., Xue, L., Wang, W., Zhang, Q., Petäjä, T., Qi, X., Gao, X., Wang, X., Yang, X., Fu, C., Kulmala, M., 2014. Polluted dust promotes new particle formation and growth.

https://doi.org/10.5194/egusphere-2024-2493
Preprint. Discussion started: 18 September 2024
© Author(s) 2024. CC BY 4.0 License.

Scientific Reports 4, 6634.

Park, T. W., Ho, C. H. Deng, Y., 2014. A synoptic and dynamical characterization of wave-train and blocking cold surge over East Asia, Climate Dynamics 43, 753–770.

Perrone, M. R., Vecchi, R., Romano, S., Becagli, S., Traversi, R., Paladini, F., 2018. Weekly cycle assessment of PM mass concentrations and sources, and impacts on temperature and wind speed in Southern Italy. Atmospheric Research 218, 129–144.

Qian, Y., Hsu, P. C., Kazuyoshi, K., 2019. New real-time indices for the quasi-biweekly oscillation over the Asian summer monsoon region. Climate Dynamics 53, 2603–2624.

Quan, J., Xu, X., Jia, X.. Liu, S., Miao, S., Xin, J., Hu, F., Wang, Z., Fan, S., Zhang, H., Mu, Y., Dou, Y., Cheng, Z., 2020. Multi-scale processes in severe haze events in China and their interactions with aerosols: Mechanisms and progresses. Chin. Sci. Bull. 65, 810–824.

Schepanski, K., Mallet, M., Heinold, B., Ulrich, M., 2016. North African dust transport toward the western Mediterranean basin: Atmospheric controls on dust source activation and transport pathways during during June–July 2013. Atmos. Chem. Phys. 16, 14147–14168.

Shen, L., Hu, W., Zhao, T., Bai, Y., Wang, H., Kong, S., Zhu, Y., 2021. Changes in the Distribution Pattern of $PM_{2.5}$ Pollution over Central China. Remote. Sens. 13, 4855.

Shen, L., Zhao, T., Liu, J., Wang, H., Bai, Y., Kong, S., Shu, Z., 2022. Regional transport patterns for heavy $PM_{2.5}$ pollution driven by strong cold airflows in Twain-Hu Basin, Central China. Atmospheric Environment 269, 118847.

Shu, Z., Liu, Y., Zhao, T., Xia, J., Wang, C., Cao, L., Wang, H., Zhang, L., Zheng, Y., Shen, L., Luo, L., Li, Y., 2021. Elevated 3D structures of $PM_{2.5}$ and impact of complex terrain-forcing circulations on heavy haze pollution over Sichuan Basin, China. Atmos. Chem. Phys. 21, 9253–9268.

Tan, Q., Ge, B., Xu, X., Gan, L., Yang, W., Chen, X., Pan, X., Wang, W., Li, J., Wang, Z., 2021. Increasing impacts of the relative contributions of regional transport on air pollution in Beijing: Observational evidence, Environmental Pollution 292, 118407.

Tao, M., Chen, L., Li, R., Wang, L., Wang, J., Wang, Z., Tang, G., Tao, J., 2016. Spatial oscillation of the particle pollution in eastern China during winter: Implications for regional air quality and climate. Atmospheric Environment, 144, 100–110.

Wang, H., Kumar, A., Murtugudde, R., Narapusetty, B., Seip, K. L., 2019. Covariations between the Indian Ocean dipole and ENSO: a modeling study. Climate Dynamics 53, 5743–5761.

Wang, J., Lu, X., Yan, Y., Zhou, L., Ma, W., 2020. Spatiotemporal characteristics of $PM_{2.5}$ concentration in the Yangtze River Delta urban agglomeration, China on the application of big data and wavelet analysis. Science of the Total Environment 724, 138134.

Wang, X., Zhang, R., Tan, Y., Yu, W., 2021. Dominant synoptic patterns associated with the decay process of $PM_{2.5}$ pollution episodes around Beijing. Atmos. Chem. Phys. 21, 2491–2508.

Wu, B., Wang, J., 2002. Winter Arctic oscillation, Siberian High and EAWM, Geophys. Res. Lett. 29, 1897.

Wu, G., Li, Z., Fu, C., Zhang, X., Huang, R., 2016. Advances in studying interactions between aerosols and monsoon in China. Sci. China. Earth. Sci. 59, 1–16.

Wu, X., He, S., Guo, J., Sun, W., 2021. A multi-scale periodic study of $PM_{2.5}$ concentration in the Yangtze River Delta of China based on Empirical Mode Decomposition-Wavelet Analysis, China. Journal of Cleaner Production 281, 124853.

Xu, C., Ma, Y., Panday, A., Cong, Z., Yang, K., Zhu, Z., Wang, J., Amatya, P. M., Zhao, L., 2014. Similarities and differences of aerosol optical properties between southern and northern sides of the Himalayas. Atmos. Chem. Phys. 14, 3133–3149.

https://doi.org/10.5194/egusphere-2024-2493
Preprint. Discussion started: 18 September 2024
© Author(s) 2024. CC BY 4.0 License.

Xu, X., Zhao, T., Liu, F., Gong, S. L., Kristovich, D., Lu, C., Guo, Y., Cheng, X., Wang, Y., and Ding, G., 2016 Climate modulation of the Tibetan Plateau on haze in China. Atmos. Chem. Phys., 16, 1365–1375.

Yang, Q., Zhao, T., Bai, Y., Wei, J., Sun, X., Tian, Z., Hu, J., Ma, X., Luo, Y., Fu, W., Yang, K., 2024. Interannual variations in ozone pollution with a dipole structure over Eastern China associated with springtime thermal forcing over the Tibetan Plateau. Science of The Total Environment, 923, 171527.

Yang, W., Li. J., Wang, Z., Wang. L., Dao, X., Zhu. L., Pan, X., Li. Y., Sun, Y., Ma. S., Wang, W., Chen. X., Wu, J., 2021. Source apportionment of $PM_{2.5}$ in the most polluted Central Plains Economic Region in China: Implications for joint prevention and control of atmospheric pollution, Journal of Cleaner Production 283, 124557.

Yang, Y., Zhou, Y., Li, K., Wang, H., Ren, L., Zeng, L., Li, H., Wang, P., Li, B., Liao, H., 2021. Atmospheric circulation patterns conducive to severe haze in eastern China have shifted under climate change. Geophysical Research Letters 48, e2021GL095011.

Yu, C., Zhao, T., Bai, Y., Zhang, L., Kong, S., Yu, X., He, J., Cui, C., Yang, J., You, Y., Ma, G., Wu, M., Chang, J., 2020. Heavy air pollution with a unique "non-stagnant" atmospheric boundary layer in the Yangtze River middle basin aggravated by regional transport of $PM_{2.5}$ over China. Atmos. Chem. Phys. 20, 7217–7230.

Zhang, Q., Zheng, Y., Tong, D., Shao, M., Wang, S., Zhang, Y., Xu, X., Wang, J., He, H., Liu, W., Ding, Y., Lei, Y., Li, J., Wang, Z., Zhang, X., Wang, Y., Cheng, J., Liu, Y., Shi, Q., Yan, L., Geng, G., Hong, C., Li, M., Liu, F., Zheng, B., Cao, J., Ding, A., Gao, J., Fu, Q., Huo, J., Liu, B., Liu, Z., Yang, F., He, K., and Hao, J., 2019. Drivers of improved $PM_{2.5}$ air quality in China from 2013 to 2017, P. Natl. Acad. Sci. USA. 116, 24463–24469.

Zhang, X., Wang, Y., Niu, T., Zhang, X., Gong, S., Zhang, Y., Sun, J., 2012. Atmospheric aerosol compositions in China: Spatial/temporal variability, chemical signature, regional haze distribution and comparisons with global aerosols. Atmos Chem Phys 12, 779–799.

Zhang, X., Xu, X., Ding, Y., Liu, Y., Zhang, H., Wang, Y., Zhong, J., 2019. The impact of meteorological changes from 2013 to 2017 on $PM_{2.5}$ mass reduction in key regions in China. Science China Earth Sciences 62, 1885–1902.

Zhang, Y., Ding, A., Mao, H., Nie, W., Zhou, D., Liu, L., Huang, X., Fu, C., 2016. Impact of synoptic weather patterns and inter-decadal climate variability on air quality in the North China Plain during 1980-2013. Atmospheric Environment, 124, 119–128.

Zhao, S., Feng, T., Tie, X., Dai, W., Zhou, J., Long, X., Li, G., Cao, J., 2019. Short-term weather patterns modulate air quality in eastern China during 2015–2016 winter. Journal of Geophysical Research: Atmospheres 124, 986–1002.

Zheng, B., Tong, D., Li, M., Liu, F., Hong, C., Geng, G., Li, H., Li, X., Peng, L., Qi, J., Yan, L., Zhang, Y., Zhao, H., Zheng, Y., He, K., Zhang, Q., 2018. Trends in China's anthropogenic emissions since 2010 as the consequence of clean air actions. Atmos. Chem. Phys., 18, 14095–14111.

Zheng, Z., Ren, G., Wang, H., Dou, J., Gao, Z., Duan, C., Li, Y., Ngarukiyimana, J. P., Zhao, C., Cao, C., Jiang, M., Yang, Y., 2018. Relationship between fine-particle pollution and the urban heat island in Beijing, China: observational evidence. Bound-Lay. Meteorol. 169, 93–113.

Zhong, J., Zhang, X., Dong, Y., Wang, Y., Liu, C., Wang, J., Zhang, Y., Che, H., 2019. Feedback effects of boundary-layer meteorological factors on cumulative explosive growth of PM2.5 during winter heavy pollution episodes in Beijing from 2013 to 2016. Atmos. Chem. Phys. 18, 247–258.

Zhu, W., Xu. X., Zheng, J., Yan. P., Wang, Y., Cai. W., 2018. The characteristics of abnormal wintertime pollution events in the Jing-Jin-Ji region and its relationships with meteorological factors. Science of the Total Environment 626, 887–898.